Research, Society and Development, v. 12, n. 4, e25912441268, 2023
(CC BY 4.0) | ISSN 2525-3409 | DOI: http://dx.doi.org/10.33448/rsd-v12i4.41268

Optimization process of vaccine production of outer membrane vesicle from *Neisseria meningitidis* associated with Zika virus

Otimização do processo de produção de vacina de vesícula de membrana externa de *Neisseria meningitidis* associada a Zika vírus

Optimización del proceso de producción de la vacuna de vesículas de membrana externa de *Neisseria meningitidis* asociada al virus del Zika

Received: 03/30/2023 | Revised: 04/12/2023 | Accepted: 04/13/2023 | Published: 04/18/2023

João Paulo de Oliveira Guarnieri[1]
ORCID: https://orcid.org/0000-0003-3098-5851
University of Campinas, Brazil
E-mail: joaopauloguarnieri@gmail.com
Bruno Gaia Bernardes[1]
ORCID: https://orcid.org/0000-0001-7631-3458
University of Campinas, Brazil
E-mail: brunogaiabernardes@gmail.com
Carlos Fernando Macedo da Silva[1]
ORCID: https://orcid.org/0000-0003-2366-6748
University of Campinas, Brazil
E-mail: nandomacedo42@gmail.com
Janaína Artem Ataide[2]
ORCID: https://orcid.org/0000-0002-1929-9474
University of Campinas, Brazil
E-mail: janaina.a.ataide@gmail.com
Arthur Noin de Oliveira[3]
ORCID: https://orcid.org/0000-0002-4451-632X
University of Campinas, Brazil
E-mail: arthurnoin95@gmail.com
Jeany Delafiori[3]
ORCID: https://orcid.org/0000-0003-2481-0465
University of Campinas, Brazil
E-mail: jeanydelafiori@gmail.com
Rodrigo Ramos Catharino[3]
ORCID: https://orcid.org/0000-0001-7219-2644
University of Campinas, Brazil
E-mail: rodrigo.catharino@fcf.unicamp.br
Priscila Gava Mazzola[2]
ORCID: https://orcid.org/0000-0002-3795-8189
University of Campinas, Brazil
E-mail: pmazzola@fcf.unicamp.br
Marcelo Lancellotti[1]
ORCID: https://orcid.org/0000-0002-4257-1034
University of Campinas, Brazil
E-mail: marcelo.lancellotti@fcf.unicamp.br

Abstract

Several vaccine prototypes were made using variations in concentration, volume, time and speed of agitation. From these prototypes, some characterization assays were carried out, such as the analysis of particle size and zeta potential, where it was possible to determine the size of the nanoparticles, the polydispersity index, with the most promising samples having a size of 252.1nm ± 71.2 nm. The polydispersity index was 0.572 ±0.02, the standard deviation being a little high due to the presence of free viral particles and some associated vesicles. It is noteworthy that the isolated vesicle has a size of 140 to 160nm and the polydispersity index of 0.513 demonstrates that we do not have

[1] LABIOTEC – Laboratory of Biotechnology, Faculty of Pharmaceutical Sciences, University of Campinas (UNICAMP), Campinas, São Paulo, Brazil
[2] LaFateCS - Laboratório de Farmacotécnica e Cuidado em Saúde, Faculty of Pharmaceutical Sciences, University of Campinas (UNICAMP), Campinas, São Paulo, Brazil
[3] INNOVARE Biomarkers Laboratory, Faculty of Pharmaceutical Sciences, University of Campinas (UNICAMP), Campinas, São Paulo, Brazil

interference in the sample of our vesicle (it is known that the size of the viral particle of Zika virus is between 40 and 60nm). Cytotoxicity testing was done to analyze whether they have cytotoxic profiles and also demonstrate that the prototype's neutralization and inactivation method works correctly. The analysis of the protein profile of some of the samples revealed that there are two major Zika virus proteins in the fused proteasome, namely the E protein, which is directly involved in the recognition of host cell receptors, and the C protein, which is related to capsid assembly, in addition to playing an important role in the immune response.
Keywords: Vaccine; OMV; Outer membrane vesicle; Zika virus; Scheduling.

Resumo
Vários protótipos de vacinas foram feitos usando variações de concentração, volume, tempo e velocidade de agitação. A partir destes protótipos, foram realizados alguns ensaios de caracterização, como a análise de tamanho de partícula e potencial zeta, onde foi possível determinar o tamanho das nanopartículas, o índice de polidispersão, tendo as amostras mais promissoras um tamanho de 252,1nm ± 71,2 nm. O índice de polidispersão foi de 0,572 ±0,02, sendo o desvio padrão um pouco alto devido à presença de partículas virais livres e algumas vesículas associadas. Vale ressaltar que a vesícula isolada tem tamanho de 140 a 160nm e o índice de polidispersão de 0,513 demonstra que não temos interferência na amostra de nossa vesícula (sabe-se que o tamanho da partícula viral do vírus Zika está entre 40 e 60 nm). O teste de citotoxicidade foi feito para analisar se eles têm perfis citotóxicos e também demonstrar que o método de neutralização e inativação do protótipo funciona corretamente. A análise do perfil proteico de algumas das amostras revelou que existem duas proteínas principais do vírus Zika no proteassoma fundido, a saber, a proteína E, que está diretamente envolvida no reconhecimento de receptores de células hospedeiras, e a proteína C, que está relacionada à montagem do capsídeo, além de desempenhar um papel importante na resposta imune.
Palavras-chave: Vacina; VME; Vesícula de membrana externa; Zika vírus; Escalonamento.

Resumen
Se han fabricado varios prototipos de vacunas utilizando variaciones en la concentración, el volumen, el tiempo y la velocidad de agitación. A partir de estos prototipos se realizaron algunas pruebas de caracterización como el análisis de tamaño de partícula y potencial zeta, donde se logró determinar el tamaño de las nanopartículas, el índice de polidispersión, siendo las muestras más promisorias con un tamaño de 252.1nm ± 71,2 nm. El índice de polidispersión fue de 0.572 ±0.02, siendo la desviación estándar un poco alta debido a la presencia de partículas virales libres y algunas vesículas asociadas. Cabe destacar que la vesícula aislada tiene un tamaño de 140 a 160nm y el índice de polidispersión de 0.513 demuestra que no tenemos interferencia en nuestra muestra de vesícula (se sabe que el tamaño de la partícula viral del virus Zika está entre 40 y 60 Nuevo Méjico). La prueba de citotoxicidad se realizó para analizar si tienen perfiles citotóxicos y también demostrar que el método de neutralización e inactivación del prototipo funciona correctamente. El análisis del perfil proteico de algunas de las muestras reveló que hay dos proteínas principales del virus del Zika en el proteasoma fusionado, a saber, la proteína E, que está directamente involucrada en el reconocimiento de los receptores de la célula huésped, y la proteína C, que está relacionada con el ensamblaje de la cápside, además de jugar un papel importante en la respuesta inmune.
Palabras clave: Vacuna; VME; Vesícula de membrana externa; Virus Zika; Escalada.

1. Introduction

Zika viruses are an arbovirus of the flaviviridae family, they are single-stranded RNA viruses, in which the RNA base sequence is identical to the messenger RNA, (+) ssRNA, and can thus be directly transcribed. The genome of Zika, like other flaviviruses, has two non-coding regions, 3'UTR and 5'UTR, which are essential for the initiation of negative strand RNA synthesis to occur in the host cell (Markoff, 2003). The remainder of the genome encodes a single precursor polyprotein, which must be processed by cellular and viral proteases to form all structural (C, M and E) and non-structural virus proteins (NS1, NS2a, NS2B, NS3, NS4A, 2K, NS4B and NS5) (Zhang et al., 2003, Lee & Shin, 2019, Labib & Chigbu, 2022, Chen et al., 2023).

The Zika virus virion is 40-60 nm in diameter, spherical in shape and has a lipid envelope (Gurumayum et al., 2018, Barreto-Vieira et al., 2016) and is vectored by female mosquitoes of the genus Aedes, of the 2 species, aegypti and albopictus; whose bite transmits the virus to humans, and these bites tend to occur mainly in the daytime, since mosquitoes of the genus Aedes have diurnal habits, especially dawn and dusk (Agumadu & Ramphul, 2018).

In 2016, the disease caused by Zika virus was declared by WHO as a public health emergency (WHO, 2016), and Brazil was considered the epicenter of the pandemic with more than 130 thousand reports of Zika virus (Amaral et al., 2019),

and with an exponential increase in cases of microcephaly and cases of neurological diseases, such as Guillain-Barré syndrome (Garcez et al., 2016, Giraldo et al., 2023).

The development of Zika vaccines began in the second half of 2015, when the genomic sequence of the virus was determined from a sample isolated in Brazil (Barrett, 2018). In 2020, some vaccines for Zika are still in phase 1 of clinical testing, that is, it is the phase in which it shows the safety of the vaccine. the ZPIV vaccines which are responsible for the companies NIAID, WRAIR and BIDMC, PZIV from Takeda, BBV121 from Bharat Biotech and VLA1601 from the companies Valneva Austria GmbH and Emergent BioSolutions, all of which use aluminum hydroxide as an adjuvant and taking in their constitution the complete virus (Barrett, 2018, Pattnaik & Pattnaik, 2020, Yeasmin et al., 2023). In addition to these 4, there are other vaccines that are also in the clinical testing phase, the vast majority of which are in phase 1, only one of the vaccines is in phase 2, which is the phase that aims to establish its immunogenicity.

2. Methodology

Bacterial strain

The strain used in this work was the *N. meningitidis* C2135, which was cultivated in GC agar at 37°C with 5% CO2 for 18-24 hours. The extraction of OMV from *N. meningitidis* was made by ultrafiltration following the descriptions of Alves et al. (2013).

Viral samples and cell lineage

Cell line Vero (African green monkey – ATCC CCL 81) was used, adapted to a temperature of 37°C, 5% CO2, maintained with RPMI 1640 medium and 10% FBS (fetal bovine serum). The Zika virus viral sample was provided by the team from the Institute of Biomedical Sciences (ICB) of the University of São Paulo (USP) and originated at the Evandro Chagas Institute located in Pará, Brazil.

Production of the vaccine prototype of Zika virus associated with the outer membrane vesicle of *Neisseria meningitidis*

The production was made based on Martins et al. (2018), where 1 ml of Zika virus was placed on the Vero cell monolayer at a concentration of $1x10^3$ and then shaken every 15 minutes for 1 minute under gentle agitation. After 1 hour of this stirring process every 15 minutes, an additional 9mL of RPMI medium was added to complete the 10mL volume in the culture bottle and then left in an oven until reaching 80% cytopathic effect in the vero cell (approximately 24-48 hours), when this effect is reached, the OMVs are then added in different concentrations and after that the culture bottle is placed for controlled agitation, for a determined time, as shown in Table 1.

Table 1 - Scheduling parameters (RPM - Revolutions per minute).

Samples	Time(hours)	RPM	Area (cm²)	Volume (ml)
8'	10	150	25	10
utip	10	50	75	30
PN	10	72	75	10
Tm	10	200	75	10

Source: Prepared by the authors.

After the stirring time is finished, the entire contents of the bottle are then filtered, without scraping the bottom of the

bottle, in a 0.22um filter and then passed to the inactivation process and subsequent storage in a ultrafreezer.

The inactivation process was done in two ways, the first physically, only heating at 56°C for 1 hour in a water bath, the other process was chemical, where formaldehyde was added at 1% of the final concentration.

Nanoparticle characterization

The mean size determines the average length of the OMVs and the polydispersity index (PDI), which is a dimensionless measure of the amplitude of the particle size distribution. The analytical procedure was performed in a Malvern (USA) Zeta-sizer Nano series ZS. Results were expressed as the mean ± standard deviation of at least three different lots of each OMV preparation. Zeta potential was determined by OMV laser Doppler Anemometry (LDA) followed by dilution in NaCl at a conductivity of approximately 120±20 S/cm^2.

The NTA (nanoparticle tracking analysis) technique allows defining the size and load of the vaccine formulations in the population percentage of the formulation. Very similar to flow cytometry, NTA allows us to characterize the size of these nanostructures and whether or not there were changes in size and residual load after several steps of the vaccine production process, viral adsorption or adjuvant. Tests with the NTA were performed on the NanoSigh device. The samples were analyzed in triplicate.

The images acquisition from cryomicroscopy and sample analysis, copper gratings for electron microscopy were used, with Lacey-type carbon film (#01895-F, Ted Pella, USA). The grids were treated with a load of 25 mA for 50 seconds, in EasiGlow equipment (TedPella, USA). Freezing in amorphous ice (cryopreparation) was performed using Vitrobot Mark IV equipment (Thermo Fischer Scientific) at controlled temperature (22 °C) and humidity (100%). Sample preparation followed the following parameters: blot time 3 seconds; blot force -5, blot wait 0, followed by a single blot. Then, 3 µL of the samples were applied to the grids and immersed in liquid ethane. After immersion, the grid was kept in liquid nitrogen until the moment of analysis under the microscope.

The images were acquired using a transmission electron microscope model Titan Krios (Thermo Fisher Scientific, USA), operating at 300kV; the microscope is equipped with a Ceta CMOS 4k x 4k camera (Thermo Fisher Scientific, USA) for digital image acquisition. Images were not processed.

Also, the protein analysis was performed using the SDS-Page gels electrophoresis for protein profile determination in all the variable samples.

For each sample group, one aliquot of the samples in culture medium was collected for Mass Spectrometry Analysis. Each sample was prepared using 20 µL of nanovesicles in culture medium, mixed with 200 µL of tetrahydrofuran (THF), followed by vortex for 30 seconds and addition of 780 µL of methanol. Then, the sample was stirred using vortexing for 30 seconds and the supernatant separated through centrifugation at 3200 rpm, for 5 min at 4°C. Fifty microliters of the supernatant were diluted in 450 µL of methanol. One microliter of formic acid was added to the final aliquot for analysis in positive ion mode through direct infusion in an ESI-LTQ-XL Discovery (Thermo Scientific, Bremen, Germany) mass spectrometer. The equipment setup was the following: flow rate of 10 µL.min^{-1}, capillary temperature at 275 °C, spray voltage of 5 kV and nitrogen sheath gas at 8 arbitrary units. A mass range of 100-1500 m/z was used for spectrum data acquisition. Each aliquot was acquired in five spectral replicates.

A heatmap was prepared using the software MetaboAnalyst 5.0 (Pang et al, 2021) to identify the presence of already validated molecules in the groups (Martins et al, 2018). Mass fragmentation experiments were performed with energies for collision-induced dissociation (CID) of 40eV using Helium as collision gas. Structural elucidation was performed using Mass Frontiers (v. 6.0, Thermo Scientific, San Jose, CA) software for comparison of experimental mass fragments to the proposed structures.

Scale up process

Bioprocess parameters (such as maintenance of nutrients, temperature, pH, oxygen demand and cell types) were used. Variable parameters used in scale up process was agitation and surface area obeying scaling constants (shear constancies, impeller power and Reynolds number) being used to guide the scale-up process. The production of the conjugate between the OMVs followed the process of cellular adsorption in which Zika virus-infected cells were shaken for different times, concentrations and speed of agitation.

From that point the following equations were used:

- $vtip = N.D \ / N_2 = N_1 \frac{D_1}{D_2}$
- $t_m = \alpha \frac{D^{0,16}}{N^{0,66}} / N_2 = N_1 . \left(\frac{D_2}{D_1}\right)^{\frac{1}{4}}$
- $Pv = N_2 = N_1 . \left(\frac{D_1}{D_2}\right)^{\frac{2}{3}}$

In these equations, the following unknowns were used, where: **N1** is the frequency of rotation of the stirrer from the initial experiment; **D1** is the area used in the first experiment; **N2** is the frequency of rotation that was found; **D2** is the area that was used in the scheduling.

3. Results

The scaling-up process made from the preparation based on the article by Martins et al. (2018) in which the size of the initial sample as well as its results in other experiments. The values used for the scaling are described in table 1.

To verify the quality of the OMV-ZIKV nanovesicles, the zetasizer nano equipment (Malvern Instruments Ltd., Grovewood Road, Malvern, UK) was used, where this equipment can measure the interaction between lipid particles as well as their electrostatic charge, and from the values obtained, it is then possible to estimate its stability among other factors, such as its ability to flocculate or aggregate. The results obtained are summarized in Table 2. The OMV-ZIKV vesicles showed in their results to be larger than the vesicles without Zika virus, in addition to the polydispersity index (PDI) being very close to 0, which reveals that there are few or no interferences in the production of the vesicles; another important factor found in the results is also the load of the OMV-ZIKV and OMV vesicles where they presented results of -0,429 ±0,29mV and -12,0 ± 1,9mV respectively).

Table 2 - Characterization by Zetasizer (PDI - polydispersity index).

Samples	size (nm)	PDI	Potencial (mV)
OMV	149,5 ± 7,8	0,513	-12,0 ± 1,9
8'	207,4 ± 51,8	0,572	-0,429 ± 0,29
utip	293,4 ± 86,2	0,417	-17,1 ± 4,8
PN	358,1 ± 59,2	0,973	-12,0 ± 0,451
Tm	298,2 ± 75,53	0,545	-16,0 ± 5,5

Source: Prepared by the authors.

Sample 8’ was used as the basis for the preparation of the other samples, as it presented the best results both in the Zeta Potential and in the characterization by NTA, becoming the best sample for the scaling process, as shown in Table 3.

Table 3 - Characterization by NTA of the nanoparticles of OMV samples, OMV/ZIKAV association (PPF - Particles per frame).

Samples	Size (nm)	D90 (nm)	Particles/ml	PPF
OMV	142,5 ± 6,2	162,4 ± 8,7	$2,67 \times 10^{8} \pm 0,0139 \times 10^{8}$	73,1 ± 0,4
8'	212,1 ± 19,2	230,3 ± 35,1	$2,27 \times 10^{8} \pm 7,62 \times 10^{7}$	13,4 ± 4,2
utip	168,9	315,6	$4,84 \times 10^{8} \pm 4,25 \times 10^{7}$	27,5
PN	169,5	311	$1,51 \times 10^{8} \pm 8,61 \times 10^{7}$	13,5
Tm	176	342	$2,75 \times 10^{8} \pm 4,69 \times 10^{7}$	18,7

Source: Prepared by the authors.

The SDS-Page was made using the same preparations we made using the sample 8’, υtip, tm and Pv. The image of the gel after the race and being stained with silver nitrate (Figure 1).

Figure 1 - Protein Gel stained with silver nitrate. On the left we have the molecular weight standard with its values, on the right the value in kDa of the protein profile of the preparations and the Zika virus.

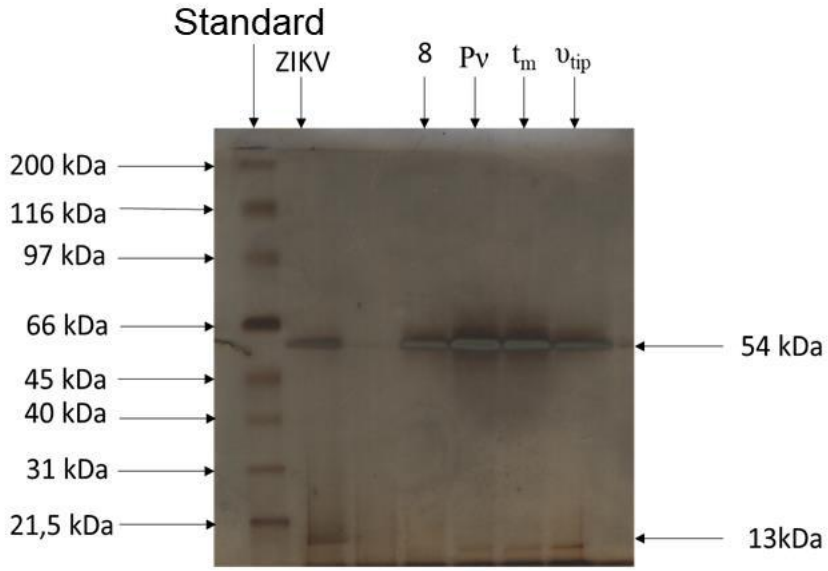

Source: Prepared by the authors.

From the HRMS it was possible to obtain the heat map and the table with its fragments (Figure 2 and Table 4) where the visualization of the values and the heat map it is possible to determine the equal regions between the samples and the OMV and the zika virus.

Figure 2 - Clustering result of 12 top features in the PLS-DA VIP scores, shown as a heat map, with a color-coded thermometer(bottom) indicating the relative presence or absence of the metabolites on each group.

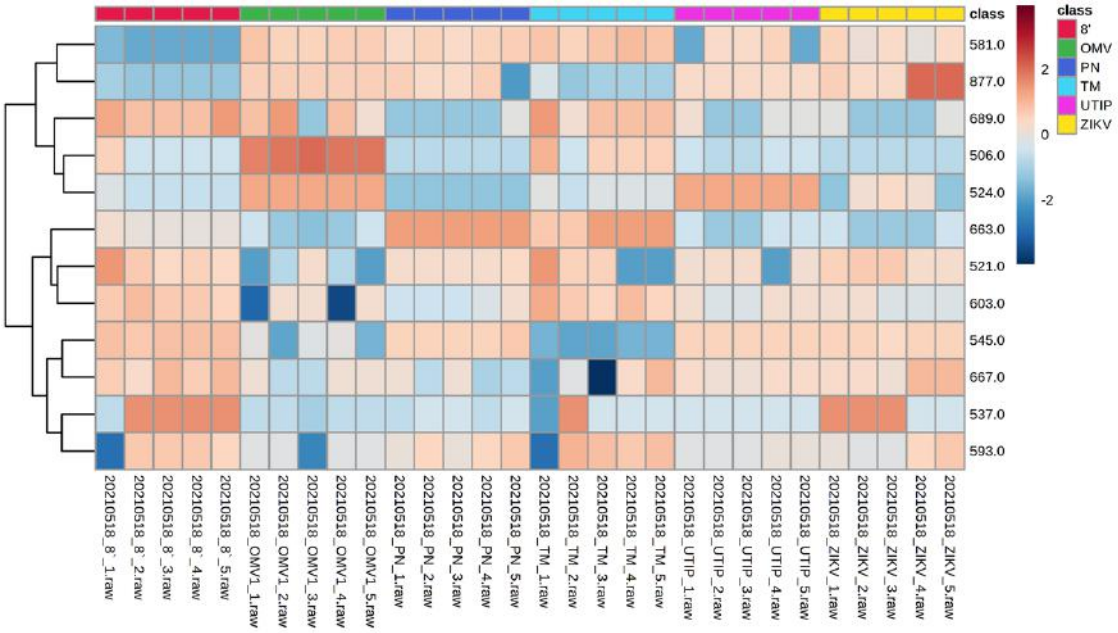

Source: Prepared by the authors.

Table 4 - Mass Fragment Table.

Experimental Mass	Theoretical Mass	Adduct	Molecule	Mass Fragments
506	506.4180	[M+Na]+	O-behenoylcarnitine	
521	521.2792	[M+H]+	dolichyl diphosphate	451 – 463 – 489 - 503
524	524.2983	[M+H]+	PS(18:1/0:0)	271 – 299 – 492 - 506
537	537.4513	[M+H]+	DG(14:1/16:1/0:0)	199 – 287 – 425 – 491
545	545.2721	[M+Na]+	14-O-(β-D-glucopyranosyl)−7S	349 – 429 – 475 - 487 - 513
581	581.5139	[M+H]+	DG(16:0/17:1/0:0)	331 – 435 – 469 - 525
593	593.2721	[M+H]+	PI(18:4/0:0)	447 – 535 – 547 – 561 - 575
603	603.3656	[M+H]+	dolichyl β-D-glucosyl phosphate	483 – 523 – 545 – 571 - 585
663	663.4959	[M+H]+	PA(14:0/19:0) and/or	481 – 543 – 617 - 645
			PA(17:0/16:0) and/or	
			PA(19:0/14:0) and/or	
			PA(16:0/17:0)	
667	667.2854	[M+Na]+	PI(22:6/0:0)	283 – 311 – 521 – 635 - 649
689	689.5115	[M+Na]+	DG(18:3/22:4/0:0)	527 – 573 – 643 – 653 – 657 - 671
851	851.5644	[M+H]+	PI(15:0/20:1) and/or	569 – 595 – 597 – 819 - 833
			PI(15:1/20:0)	
877	877.5801	[M+H]+	PI(17:0/20:2) and/or	595 – 819 – 845 - 859
			PI(17:1/20:1) and/or	
			PI(17:2/20:0)	

Source: Prepared by the authors.

The cryomicroscopy performed allowed us to observe the OMV image and what would be the possible association of the OMV with the Zika virus looks like (Figure 3).

Figure 3 - Cryomicroscopy. (a) Cryomicroscopy of Zika virus. (b) cryomicroscopy of OMV. (c) Cryomicroscopy of OMV/ZIKAV association. The size increasing of the nanoparticle showed when comparing the figure (c) with the figures (a) and (b).

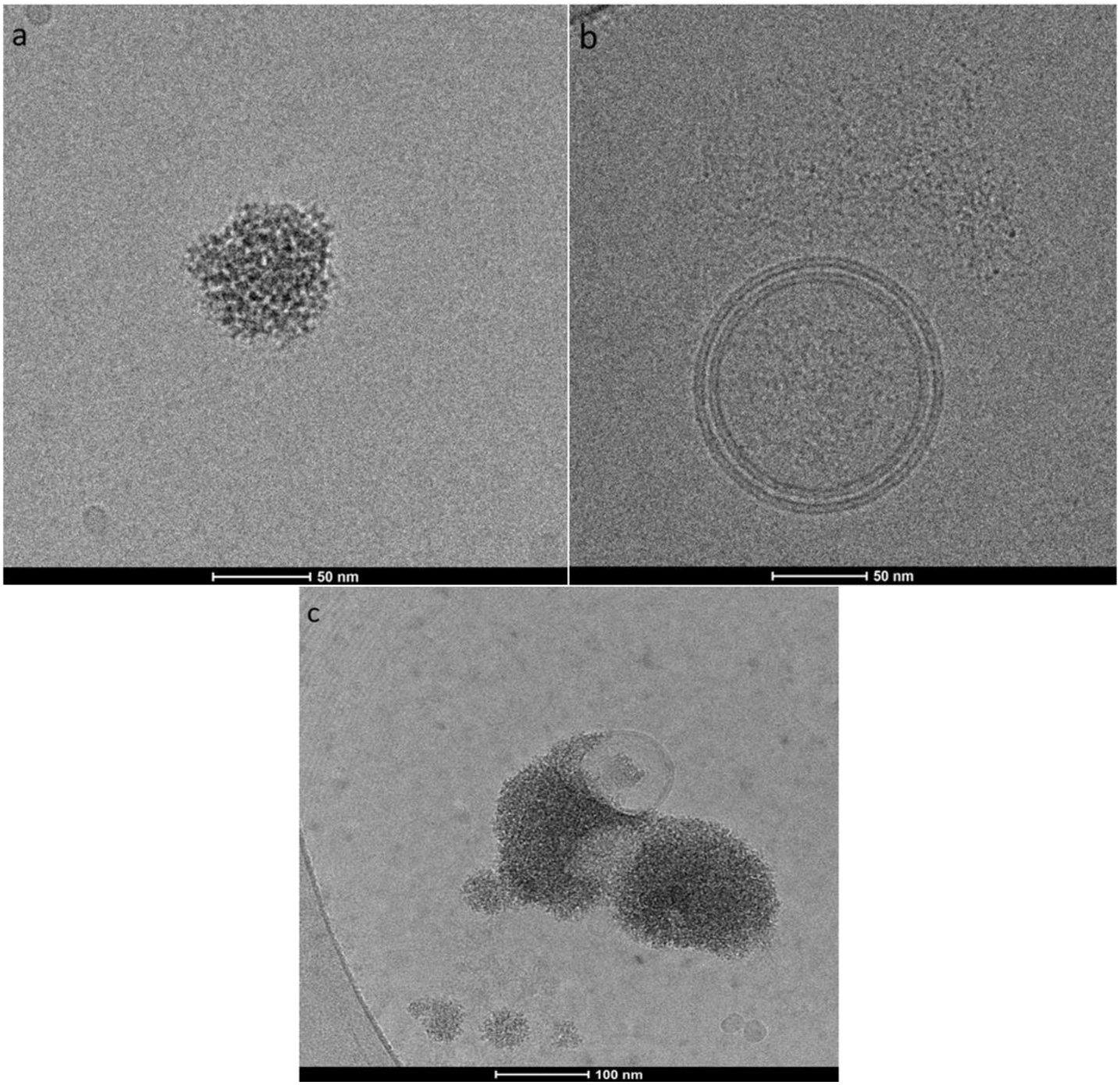

Source: Prepared by the authors.

4. Discussion

The size of the OMVs as demonstrated in the results obtained is within the size standard for Neisseria OMVs described by Van der Pol et al.(2015); from this data and knowing that Zika virus is 40-60 nm in diameter, spherical in shape and lipid envelope (Gurumayum et al., 2018, Barreto-Vieira et al., 2016) we then arrived at the size comparison from the fusion described by Martins et al. (2018) where it is possible to say that we have the size of the fused particles similar to those

obtained previously, having said that, the result obtained in zeta-sizer and NTA is bigger than just OMV and also Zika virus, showing an increase in size after fusion of both. In this case, based on the values obtained, it was observed that the average size of this sample is on average above 200 nm, which shows that a possible fusion occurred between the particles. The variation of factors in the preparation of these samples showed the possibility of scaling up based on the equation of utip, Pn and tm.

The results obtained from the characterization of the new nanoparticles associated with Zika virus (Table 2) kept the polydispersity index (PDI) close to 0, and the potential values had a slight increase, reaching -17mV, which could help to maintain product stability.

As we could see in the protein profile in the molecular weight standard, and compared to the Zika virus band, we came to the conclusion that the size of this band is approximately 54kDa, evidencing that we have the E protein very well expressed in the sample, this E protein is the main protein surface of flaviviruses, this protein being involved in the recognition of host cell receptors, virus entry process and viral assembly (Cruz-Oliveira et al., 2015) in addition to having an important role in the immune response, representing the main target of neutralizing antibodies (Dai et al., 2016).

In this result, we can also see another band in Zika virus around 13kDa, this protein profile is from protein C which is an extremely basic protein and is directly related to the assembly of the zika virus capsid and its incorporation into the particles of the virus in formation, in addition to being a protein with a characteristic that penetrates into cells, that is, this protein has the characteristic of being able to cross the RNA through cell membranes (van der Pol et al., 2015, Roby et al., 2015).

Based on the heat map obtained from HRMS, it is possible to analyze that Zika virus has markers different from those of OMV, while samples in which OMV is associated with Zika virus we see these markers of both OMV and Zika present in the heat map. These markers are well evidenced in the Figure 2, where we have the OMV in the bands of 689.0, 506.0 and 524.0 while the Zika virus is more evident in the bands of 545.0, 667.0, 537.0 and 593.0. In view of these ranges, we can say that in the analyzed samples all have these markers, but in some these markers are more evident, as is the case of the utip and the 8' sample. In addition, it is also possible to see through table 4 the identification of the molecules obtained through the HRMS of both OMV and Zika virus.

Furthermore, cryomicroscopy allowed us to see what really happens between OMVs and zika virus, since in the image shown, we can see zika virus, OMV and the junction of OMV and zika virus; which shows us that Zika virus associated with the membrane but Zika does not enter this vesicle.

5. Conclusion

The implementation of scale-up techniques made it possible to reach results in which the vaccine preparation before without standardization and without specific values, now has an equation that makes this scale-up and possible production on a larger scale possible. In addition, the formulation proved to be safe and completely inactivated, but presenting in its composition the main proteins of the Zika virus, the same ones that are important for its immunogenicity. In future studies we intend to isolate proteins E and C, using a plasmid to introduce them into N. meningitidis, where it would then be possible as proteins to be expressed in the bacterial membrane, and possibly be present in OMV, which would lead to future vaccine prototype for Zika virus.

Acknowledgments

Thanks for Prof. Dr. Eneida de Paula for use of NTA equipment (FAPESP 2014/14457-5). The authors would like to thank LNNano/CNPEM for the access to the electron microscopy facility and technical support in the execution of the proposal TEM-27260. Thanks to CAPES (Coordenação de Aperfeiçoamento de Pessoal de Nível Superior – Brasil) 88887.643019/2021-00 J.P.O.G. and 88881.506966/2020-01 M.L.

References

Agumadu, V. C., & Ramphul, K. (2018). Zika Virus: A Review of Literature. *Cureus*, 10(7), e3025. https://doi.org/10.7759/cureus.3025

Alves, D.A., Mattos, I.B., Hollanda, L.M., & Lancellotti, M. (2013). Use of Mesoporous Silica SBa-15 and SBa-16 in Association of Outer Membrane Vesicles - OMV from Neisseria meningitidis. *Journal of Vaccines and Vaccination*, 2013, 1-6.

Amaral P., Resende de Carvalho L., Hernandes Rocha T.A., da Silva N.C. & Vissoci J.R.N. (2019) Geospatial modeling of microcephaly and zika virus spread patterns in Brazil. *PLOS ONE* 14(9): e0222668.

Barrett, A.D.T. (2018) Current status of Zika vaccine development: Zika vaccines advance into clinical evaluation. npj *Vaccines* 3, 24.

Barreto-Vieira, D. F., Barth, O. M., Silva, M. A. N. da., Santos, C. C., Santos, A. da S., F Filho, J. B., & Filippis, A. M. B. de. (2016). Ultrastructure of Zika virus particles in cell cultures. Memórias Do Instituto Oswaldo Cruz, 111(Mem. Inst. Oswaldo Cruz, 2016 111(8)), 532–534. https://doi.org/10.1590/0074-02760160104

Chen, Y., Chi, X., Zhang, H., Zhang, Y., Qiao, L., Ding, J., Han, Y., Linm Y. & Jiang, J. (2023). Identification of Potent Zika Virus NS5 RNA-Dependent RNA Polymerase Inhibitors Combining Virtual Screening and Biological Assays. *International Journal of Molecular Sciences*, 24(3), 1900. MDPI AG. http://dx.doi.org/10.3390/ijms24031900

Cruz-Oliveira, C., Freire, J. M., Conceição, T. M., Higa, L. M., Castanho, M. A., & Da Poian, A. T. (2015). Receptors and routes of dengue virus entry into the host cells. *FEMS microbiology reviews*, 39(2), 155–170. https://doi.org/10.1093/femsre/fuu004

Dai, L., Song, J., Lu, X., Deng, Y. Q., Musyoki, A. M., Cheng, H., Zhang, Y., Yuan, Y., Song, H., Haywood, J., Xiao, H., Yan, J., Shi, Y., Qin, C. F., Qi, J., & Gao, G. F. (2016). Structures of the Zika Virus Envelope Protein and Its Complex with a Flavivirus Broadly Protective Antibody. *Cell host & microbe*, 19(5), 696–704. https://doi.org/10.1016/j.chom.2016.04.013

Garcez, P. P., Loiola, E. C., Madeiro da Costa, R., Higa, L. M., Trindade, P., Delvecchio, R., Nascimento, J. M., Brindeiro, R., Tanuri, A., & Rehen, S. K. (2016). Zika virus impairs growth in human neurospheres and brain organoids. *Science* (New York, N.Y.), 352(6287), 816–818. https://doi.org/10.1126/science.aaf6116

Giraldo, M. I., Gonzalez-Orozco, M., & Rajsbaum, R. (2023). Pathogenesis of Zika Virus Infection. *Annual review of pathology*, 18, 181–203. https://doi.org/10.1146/annurev-pathmechdis-031521-034739

Gurumayum, S., Brahma, R., Naorem, L. D., Muthaiyan, M., Gopal, J., & Venkatesan, A. (2018). ZikaBase: An integrated ZIKV- Human Interactome Map database. *Virology*, 514, 203–210. https://doi.org/10.1016/j.virol.2017.11.007

Labib, B. A., & Chigbu, D. I. (2022). Pathogenesis and Manifestations of Zika Virus-Associated Ocular Diseases. *Tropical Medicine and Infectious Disease*, 7(6), 106. MDPI AG. http://dx.doi.org/10.3390/tropicalmed7060106

Lee, J., & Shin, O. (2019). Advances in Zika Virus–Host Cell Interaction: Current Knowledge and Future Perspectives. *International Journal of Molecular Sciences*, 20(5), 1101. MDPI AG. http://dx.doi.org/10.3390/ijms20051101

Markoff, L. (2003) 5′-and 3′-noncoding regions in Flavivirus RNA. ISSN 0065-3527

Martins, P., Machado, D., Theizen, T. H., Guarnieri, J. P. O., Bernardes, B. G., Gomide, G. P., Corat, M. A. F., Abbehausen, C., Módena, J. L. P., Melo, C. F. O. R., Morishita, K. N., Catharino, R. R., Arns, C. W., & Lancellotti, M. (2018). Outer Membrane Vesicles from Neisseria Meningitidis (Proteossome) Used for Nanostructured Zika Virus Vaccine Production. *Scientific reports*, 8(1), 8290. https://doi.org/10.1038/s41598-018-26508-z

Pang, Z., Chong, J., Zhou, G., Morais D., Chang, L., Barrette, M., Gauthier, C., Jacques, PE., Li, S., and Xia, J. (2021) MetaboAnalyst 5.0: narrowing the gap between raw spectra and functional insights Nucl. *Acids Res.* (doi: 10.1093/nar/gkab382)

Pattnaik, A., Sahoo, B. R., & Pattnaik, A. K. (2020). Current Status of Zika Virus Vaccines: Successes and Challenges. *Vaccines*, 8(2), 266.

Roby, J. A., Setoh, Y. X., Hall, R. A., & Khromykh, A. A. (2015). Post-translational regulation and modifications of flavivirus structural proteins. *The Journal of general virology*, 96(Pt 7), 1551–1569. https://doi.org/10.1099/vir.0.000097

van der Pol, L., Stork, M., & van der Ley, P. (2015). Outer membrane vesicles as platform vaccine technology. *Biotechnology journal*, 10(11), 1689–1706. https://doi.org/10.1002/biot.201400395

World Health Organization. The history of zika virus (2016). https://www.who.int/news-room/feature-stories/detail/the-history-of-zika-virus

Yeasmin M., Molla M.M.A., Masud H.M.A.A., Saif-Ur-Rahman K.M. (2023) Safety and immunogenicity of Zika virus vaccine: a systematic review of clinical trials. *Rev Med Virol;* 33(1): e2385. https://doi.org/10.1002/rmv.2385

Zhang, Y., Corver, J., Chipman, P. R., Zhang, W., Pletnev, S. V., Sedlak, D., Baker, T. S., Strauss, J. H., Kuhn, R. J., & Rossmann, M. G. (2003). Structures of immature flavivirus particles. *The EMBO journal*, 22(11), 2604–2613. https://doi.org/10.1093/emboj/cdg270